B-Cell Lymphoma With Hyaline Vascular Castleman Disease–Like Features

A Clinicopathologic Study

Imran N. Siddiqi, MD, PhD,[1] Russell K. Brynes, MD,[1] and Endi Wang, MD, PhD[2]

Key Words: B-cell lymphoma; Castleman disease; Hyaline deposits; Vascular proliferation; Differential diagnosis; Follicular lymphoma; Mantle cell lymphoma; Nodal marginal zone lymphoma

DOI: 10.1309/AJCPF5AESY7OWIXF

Upon completion of this activity you will be able to:
- list the overlapping histologic features between classic hyaline vascular Castleman disease (HV-CD) and B-cell lymphomas with HV-CD–like features.
- determine histologic and clinical clues that should raise suspicion for B-cell lymphoma in cases otherwise morphologically compatible with HV-CD.
- discuss the immunohistochemical, genetic, and molecular studies that can be performed to evaluate cases of possible B-cell lymphoma with HV-CD–like features, and decide when these studies should be utilized to avoid a misdiagnosis.

The ASCP is accredited by the Accreditation Council for Continuing Medical Education to provide continuing medical education for physicians. The ASCP designates this educational activity for a maximum of 1 *AMA PRA Category 1 Credit*™ per article. This activity qualifies as an American Board of Pathology Maintenance of Certification Part II Self-Assessment Module.

The authors of this article and the planning committee members and staff have no relevant financial relationships with commercial interests to disclose.

Questions appear on p 976. Exam is located at www.ascp.org/ajcpcme.

Abstract

Hyaline vascular Castleman disease (HV-CD) is a localized benign mass characterized by follicular hyperplasia with atrophic germinal centers, mantle zone hyperplasia, hyaline deposits, and vascular proliferation. Before establishing a diagnosis of CD, several B-cell lymphomas (BCLs) must be considered, including follicular lymphoma (FL), mantle cell lymphoma (MCL), and nodal marginal zone lymphoma (NMZL). Conversely, BCLs with prominent atrophic germinal centers and hyaline vascular penetration may closely resemble HV-CD, leading to misdiagnosis. We report 6 cases of BCL with prominent HV-CD–like features, including FL (2 cases), MCL, NMZL (2 cases), and interfollicular large B-cell lymphoma. Histologically, all were initially considered to be HV-CD before additional tests revealed a neoplastic B-cell proliferation. We highlight the clinicopathologic features of these cases in comparison with cases diagnostic of HV-CD. In contrast with HV-CD, BCLs with HV-CD–like features are more likely to manifest clinically with systemic symptoms or generalized lymphadenopathy. Careful histopathologic examination, supported with immunohistochemical studies, flow cytometric immunophenotyping, and judicious use of cytogenetic and molecular analyses, allows identification of the masked neoplastic process. A multifaceted approach, integrating clinical, histologic, and ancillary tests, can help avoid this diagnostic pitfall.

Castleman disease (CD), also known as angiofollicular or giant lymph node hyperplasia, was first described more than 50 years ago as benign, localized mediastinal lymphadenopathy, histologically characterized by follicular hyperplasia and marked capillary proliferation with endothelial hyperplasia.[1] Subsequently, CD was expanded to represent a diverse group of nonneoplastic lymphoproliferative disorders involving a variety of nodal and extranodal sites with various histologic patterns.[2]

CD is classified essentially as 2 types, the hyaline vascular (HV) and plasma cell (PC) variants, based on the histopathologic features. HV-CD, the originally described classical form, constitutes 80% to 90% of CD cases. Histologically, it is characterized by increased lymphoid follicles with atrophic germinal centers, lymphocyte depletion, hyaline deposits, radially penetrating capillaries ("lollipop" follicles), surrounding concentric layers of mantle zone lymphocytes ("onion skin" pattern), and interfollicular vascular proliferation. In contrast, the PC-CD variant (10%-20% of CD cases) features mostly hyperplastic follicles, as opposed to regressed follicles, and a marked proliferation of plasma cells in the interfollicular area. Clinically, CD is also heterogeneous, ranging from asymptomatic, localized disease (most often seen in HV-CD) to systemic disease with fever, anemia, and hypergammaglobulinemia (typical of PC-CD). Nevertheless, HV-CD and PC-CD can exhibit considerable clinical and histologic overlap, and a so-called mixed variant of CD is occasionally seen. Multicentric CD, which occurs most often in PC-CD, is frequently associated with human herpesvirus-8 (HHV-8),

especially in HIV+ patients, and demonstrates elevated levels of interleukin 6. The pathogenesis of the HV variant is not entirely clear, but it may be related to genetic alterations in follicular dendritic cells.[3]

Although CD is inherently a nonneoplastic process, an association with concurrent or subsequent lymphoma has been well described.[4-6] This occurs most often with the multicentric/PC variant, and the associated lymphomas can be of the non-Hodgkin or Hodgkin type. In contrast, lymphoma arising after a diagnosis of HV-CD is uncommon, and the coexistence of lymphoma in the same lymph node or tissue site is extremely rare.

We report 6 cases of B-cell lymphoma with prominent HV-CD–like histologic features. The HV-CD–like changes in these cases were so prominent and well formed that the underlying neoplastic processes were masked, leading to a potential diagnostic error. These B-cell lymphomas span a spectrum of subtypes, including follicular lymphoma (FL), nodal marginal zone lymphoma (NMZL), focal interfollicular large B-cell lymphoma (LBCL), and mantle cell lymphoma (MCL). We highlight the clinicopathologic features of these cases in comparison with cases diagnostic of HV-CD and emphasize that HV-CD–like lymphoid proliferations should be evaluated cautiously, often with a variety of ancillary tests, to establish the correct diagnosis.

Materials and Methods

Case Selection

We retrieved cases of B-cell lymphoma with prominent HV-CD–like changes in our pathology databases by using the search terms “Castleman” and “lymphoma” in diagnostic reports for an 8-year period. Four cases were from Duke University Medical Center, Durham, NC, and 2 were from consultation material sent to the University of Southern California, Los Angeles. Cases with focal HV germinal centers within an otherwise morphologically and immunophenotypically apparent lymphoma were identified but were excluded from this study. During the search, cases diagnostic of HV-CD were also obtained and analyzed in parallel with cases of B-cell lymphoma with HV-CD–like features.

Histologic and Immunohistochemical Studies

Lymph nodes and other tissue were fixed in formalin or B-5. All specimens were then processed routinely, embedded in paraffin, sectioned, and stained with H&E. We immunostained 4-μm sections from paraffin-embedded blocks with each antibody: CD21 (dilution 1:20; DAKO, Carpinteria, CA), CD23 (dilution 1:40; DAKO), CD79a (dilution 1:100; DAKO), PAX5 (dilution 1:50; Biocare Medical, Concord, CA), OCT2 (dilution 1:500; Santa Cruz, Santa Cruz, CA), BOB.1 (dilution 1:250; Santa Cruz), CD3 (dilution 1:100; Lab Vision, Fremont, CA), CD5 (dilution 1:40; Novocastra, Newcastle upon Tyne, England), CD2 (dilution 1:20; Novocastra), CD4 (dilution 1:20; Novocastra), CD8 (dilution 1:25; DAKO), CD45RO (dilution 1:50; DAKO), CD43 (dilution 1:3,000; D-B Pharma, Saint-Amant-Tallende, France), CD10 (dilution 1:25; Novocastra), BCL6 (dilution 1:20; DAKO), BCL2 (dilution 1:50; DAKO), CD138 (dilution 1:100; DAKO), κ light chain (polyclonal antibody, DAKO), λ light chain (polyclonal antibody, DAKO), cyclin D1 (dilution 1:50; Lab Vision), CD30 (dilution 1:50, DAKO), IgG4 (dilution 1:50; Invitrogen, Carlsbad, CA), HHV-8-LNA (dilution 1:25; Novocastra), and Ki-67 (dilution 1:50; DAKO), using the streptavidin-biotin complex method. The corresponding positive and negative control slides for each antibody stain were carefully examined for quality assurance purposes.

Epstein-Barr Virus–Encoded RNA In Situ Hybridization

Epstein-Barr virus (EBV)-encoded RNA (EBER) was detected by in situ hybridization (ISH). The paraffin-embedded tissue sections were dewaxed in xylene, treated with Proteinase K, and hybridized with fluorescein-conjugated EBER oligonucleotide probe (Novocastra, Newcastle upon Tyne, England). The slides were incubated with anti–fluorescein isothiocyanate/alkaline phosphatase and then covered with 5-bromo-4-chloro-3-indolylphosphate, nitroblue tetrazolium, and 1 mol/L levamisole hydrochloride. A negative control probe consisting of a fluorescein-labeled oligonucleotide cocktail in hybridization solution was used in parallel. A known EBER ISH+ tissue section was used as a positive control. The stained sections were examined under light microscopy, and a positive cell was determined by its unequivocal nuclear staining.

Flow Cytometric Analysis

Flow cytometric immunophenotyping was performed on fresh tissue specimens collected in RPMI 1640 culture medium. Specimens were processed routinely to generate single-cell suspensions, which were then stained with premixed, 4-fluorochrome-conjugated antibodies (fluorescein isothiocyanate, phycoerythrin, peridinin chlorophyll protein, and allophycocyanin) per routine leukemia/lymphoma panel protocols. The antibodies in the panel include those against leukocyte common antigen CD45, B-cell antigens (CD19, CD20, CD22, and κ and λ light chains), T-cell antigens (CD2, CD3, CD4, CD5, CD7, and CD8), myeloid antigens (CD11c, CD13, CD14, CD15, CD33, and CD117), stem cell antigens (CD34 and CD123), and CD10, CD16, CD25, CD38, CD56, CD103, and HLA-DR (Becton Dickinson Biosciences, San Diego, CA). Approximately 10,000 events

DOI: 10.1309/AJCPF5AESY7OWIXF

per tube were acquired on a flow cytometer (dual-laser FACSCalibur, Becton Dickinson Biosciences) and analyzed using the CellQuest computer software program (Becton Dickinson Biosciences).

Interphase Fluorescence ISH

Fluorescence ISH for IGH/BCL2

An interphase fluorescence ISH (FISH) analysis was performed on the formalin-fixed, paraffin-embedded sections or on air-dried bone marrow aspirate smears using the Vysis (Downers Grove, IL) dual-color, dual-fusion probe for the immunoglobulin heavy chain (*IGH*)/*BCL2* fusion gene. This probe is designed to detect the juxtaposition of the *IGH* locus and *BCL2* gene sequences. The translocation involving *IGH* at 14q32 and *BCL2* at 18q21, t(14;18)(q32;q21), is visible by fusion of the red probe and the green probe.

FISH for CCND1/IGH

The Vysis dual-color dual-fusion *CCND1/IGH* (11;14) translocation probe set was applied to formalin-fixed, paraffin-embedded sections. This probe set is specific for sequences on either side of the *IGH* J region breakpoint (14q32) and for regions flanking the common breakpoint region (major translocation cluster) that lies centromeric to the *CCND1* locus (11q13). The translocation involving *CCND1* at 11q13 and *IGH* at 14q32, t(11;14)(q13;q32), is visible by fusion of the red probe and the green color probe.

FISH for BCL6 *and* MALT1 *Rearrangement*

Vysis dual-color "break-apart" probes for the *BCL6* or *MALT1* (18q21) locus were applied to formalin-fixed, paraffin-embedded sections. Rearrangement of *BCL6* or *MALT1* with a variety of translocation partners was visible by separation of red probes from green probes.

In total, 200 interphase nuclei were evaluated by 2 technologists, and the percentage of positive cells was reported for all FISH studies.

IGH Gene Rearrangement Studies

An assay using polymerase chain reaction (PCR)-mediated amplification of the variable (V) and joining (J) regions was used to assess *IGH* gene rearrangements. Briefly, genomic DNA extracted from the paraffin-embedded tissues was subjected to 2 independent PCR reactions targeting framework 1 and 3 sequences within the V region. Following the PCR amplification, fluorescence-labeled PCR products were resolved by capillary electrophoresis on an ABI 310 Genetic Analyzer and evaluated by using GeneMapper software (Applied Biosystems, Foster City, CA).

Results

The clinical and pathologic features of the 6 cases of B-cell lymphoma with HV-CD–like changes are summarized in **Table 1**; **Table 2** lists the clinical and ancillary test findings in comparison with 23 cases diagnostic of HV-CD. The diagnoses of B-cell lymphoma were confirmed according to the 2008 World Health Organization classification,[7-9] and the diagnoses of HV-CD were established by characteristic histologic features and pathologic exclusion of lymphoma.

Clinical Features

Among the 6 cases of B-cell lymphoma with HV-CD–like features, 4 patients were men and 2 were women. Ages ranged from 40 to 86 years with a median age of 69 years. None of the patients had a known history of congenital or acquired immunodeficiency or autoimmune disease. Of the 6 cases, 4 (cases 1, 3, 5, and 6) were de novo, and 2 (cases 2 and 4) represented relapsed disease, with the HV changes appearing at the time of recurrence.

In case 2, the patient had a history of low-grade FL 7 years earlier that was treated with 6 cycles of rituximab (R) with cyclophosphamide, doxorubicin, vincristine, and prednisolone (CHOP), with complete remission. In case 4, the patient had a history of B-cell lymphoma diagnosed by a left cervical lymph node biopsy 8 years earlier and treated with CHOP, with complete remission. All patients, except in case 4, had systemic symptoms, including fatigue and weight loss; the patient in case 4 was essentially asymptomatic, with extensive cervical lymphadenopathy and some retroperitoneal lymphadenopathy noted on a routine follow-up examination. In addition, all patients showed multifocal lymphadenopathy or involvement of other tissue sites in staging at the time of lymphoma diagnosis. At diagnosis, cases 1, 2, and 3 had stage IV disease, cases 4 and 6 had stage III disease, and case 5 had stage II disease. Among these cases, 2 biopsies were from cervical lymph nodes and 4 were from other lymph node sites.

Among the 23 cases of diagnostic HV-CD, 10 patients were male and 13 were female. Ages ranged from 11 to 85 years with a median of 25 years. In 5 patients (22%), there was a clinical history of asthma, 4 other patients (17%) had autoimmune disease, and the remaining 14 (61%) had an unremarkable clinical history or did not have clinical information detailed. Of the 23 patients, 17 (74%) had isolated lymphadenopathy or mass lesions without symptoms, and the remaining 6 (26%) had symptoms or complaints related to regional compression by the massive enlargement of internal lymph nodes (abdominal pain in a case of mesenteric lymphadenopathy) or mediastinal (thymic) lesions (chest pain, cough). The unicentric manifestation of lymphadenopathy or mass lesions involved a cervical lymph

DOI: 10.1309/AJCPF5AESY7OWIXF

Table 1
Summary of Clinicopathologic Features in B-cell Lymphomas With HV-CD–Like Features

	Case No.			
	1	**2**	**3**	**4**
Sex/age (y)	M/40	M/72	M/70	F/86
Clinical manifestations	WL; LN; splenomegaly; paraprotein	Sciatic pain; LN	WL	LN
History	No	FL (7 y); R-CHOP	Chronic illness; alcohol abuse	BCL (8 y); CHOP
Biopsy site	Cervical LN	Mesenteric LN	Axillary LN	Cervical LN
Histologic features				
Atrophic GC	+ LC	+ LC	+	+ LC
Hyaline deposits	+	+	+	+
Vascular proliferation	+	+	+	+
Intact mantle zone	+	+	+, concentric	+
Interfollicular area/ vascularity	Increased with plasmacytosis	Increased with plasmacytosis	Increased sinus histiocytosis	Increased with plasmacytosis
Initial consideration	CD	CD/FL	CD	CD/FL
Neoplastic component highlighted by IHC	Large cells in GC (B-cell+, BCL2+)	Large cells in GC (B-cell+, BCL2–)	Expanded mantle zone (cyclin D1+)	Marginal zone with follicular colonization (B-cell+, MUM1+)
Flow cytometry	–*	+ (CD10+)	+ (CD5+)	–
IGH rearrangement	Indeterminate	ND	ND	Clonal
Interphase FISH	Positive for *BCL6* rearrangement; negative for *IGH/BCL2*	Positive for *IGH/BCL2*†	Positive for *CCND1/IGH*	Trisomy 3 and 18‡
Diagnosis	FL, G3A*	FL, G3A	MCL	NMZL
Stage	IV	IV	IV	III
Treatment	R-CHOP	Rituximab	No	Supportive
Follow-up (mo)	36	4	Unknown	5
Outcome	Remission, 3 y; recent relapse with DLBCL	AWD	Unknown	AWD

AWD, alive with disease; BCL, B-cell lymphoma; CD, Castleman disease; DLBCL, diffuse large B-cell lymphoma; FISH, fluorescence in situ hybridization; FL, follicular lymphoma; G3A, grade 3A; GC, germinal center; HV, hyaline vascular; *IGH*, immunoglobulin heavy chain gene; IHC, immunohistochemical analysis; LBCL, large B-cell lymphoma; LC, large cells; LN, lymphadenopathy (clinical manifestation and outcome)/enlarged lymph nodes (biopsy site); MCL, mantle cell lymphoma; MZL, marginal zone lymphoma; ND, not done; NMZL, nodal marginal zone lymphoma; R-CHOP, rituximab, cyclophosphamide, doxorubicin, vincristine, and prednisolone; R-CVP, rituximab, cyclophosphamide, vincristine, and prednisolone; WL, weight loss; +, positive or present; –, negative or absent;
* The case was initially diagnosed as HV-CD, largely owing to a negative flow cytometric result. The case was retrospectively reevaluated when a biopsy of recurrent cervical lymphadenopathy detected a monoclonal B-cell population with CD10.
† A low level of *IGH/BCL2* was detected in a staging bone marrow biopsy specimen. Lymph node biopsy was not available for the test.
‡ No *IGH/BCL2* fusion, rearranged *MALT1*, or rearranged *BCL6* was detected; instead, 3 copies of *BCL2*, *MALT1*, and *BCL6* were seen in 14% to about 33% of interphase cells, suggesting trisomy 3 and trisomy18.

Table 2
Clinicopathologic Findings in BCL With HV-CD–Like Features and Diagnostic HV-CD*

	BCL/HV-CD Features (n = 6)	**Diagnostic HV-CD (n = 23)**
Median (range) age (y)	69 (40-86)	25 (11-85)
Sex (M/F)	4/2	10/13
Symptoms	5 (83)	6 (26)
Index lymph node or lesion		
Cervical node	2 (33)	8 (35)
Mediastinal mass	0 (0)	6 (26)
Other nodes/tissue sites	4 (67)	9 (39)
Other involvement	6 (100)	0/16 (0)
Positive flow cytometry	3 (50)	0/12 (0)
IGH rearrangement	2/3 (67)	0/4 (0)
Fluorescence in situ hybridization	3/4 (75)	—

BCL, B-cell lymphoma; HV-CD, hyaline vascular Castleman disease; *IGH*, immunoglobulin heavy chain gene.
* Data are given as number (percentage) or number/total (percentage) unless otherwise indicated.

node in 8 cases (35%), a mediastinal mass in 6 cases (26%), and various other lymph nodes or tissue sites in the remaining 9 cases (39%). In 16 cases (70%), there was radiologic imaging information available, and all demonstrated no evidence of lymphadenopathy or extranodal tissue involvement other than the index lesions.

Histologic Features

All 6 cases of B-cell lymphoma with HV-CD–like changes demonstrated increased lymphoid follicles, most of which were regressed with hyaline deposits within germinal centers, vascular proliferation, intact mantle zones, and an increase in interfollicular vascularity, features characteristically associated with HV-CD **Image 1**. Although all cases exhibited intact mantle zones, an expanded mantle zone with concentric arrangement ("onion-skinning") of mantle cells around atrophic follicles was particularly pronounced in case 3 (MCL; Image 1C). Of note, cases 3 and 5 demonstrated expansion of monomorphic lymphocytes with clear cytoplasm around atrophic germinal centers into the perifollicular zones.

DOI: 10.1309/AJCPF5AESY7OWIXF

Case No.	
5	**6**
F/68	M/60
WL; LN	WL
No	No
Groin LN	Intra-abdominal mass
+	+
+	+
+	+
+	+
Increased with sinus histiocytosis	Increased with fibrosis
CD/MZL	CD
Expanded marginal zone (B-cell+)	Interfollicular focal large cells (B-cell+)
+	–
ND	Clonal
Negative for *CCND1/IGH*	ND
NMZL	Focal LBCL
II	III
Rituximab, then R-CVP	CHOP
3	23
Subjective improvement; decreased LN	Clinical remission

Sinuses were inconspicuous to patent (Images 1C and 1E). Interfollicular plasma cells varied from absent or minimally increased in cases 3, 5, and 6 to moderately or markedly increased in cases 1, 2, and 4. Nevertheless, a confluence of plasma cells in the interfollicular areas, as typically seen in HV-CD, was not noted in these cases. In cases 1, 3, 5, and 6, the morphologic features were sufficiently developed to favor a diagnosis of HV-CD on initial examination. Owing to histories of lymphoma in cases 2 (Image 1B) and 4 (Image 1D), more thorough evaluation and ancillary workup were performed to exclude the possibility of recurrent disease, even though features of HV-CD were clearly present.

Despite the resemblance to HV-CD, most cases also showed subtle histologic deviations suggestive of an additional pathologic process. In cases 1 and 2 (FL), close inspection of the atrophic follicle centers revealed large lymphoid cells (Image 1A) **Image 2A**, but it was difficult to distinguish these from follicular dendritic cells, particularly dysplastic dendritic cells, by morphologic examination alone. Case 4 (NMZL) demonstrated, on higher magnification, clusters of large lymphoid cells in follicle centers and focally expanded interfollicular areas with increased numbers of large cells admixed with small lymphocytes **Image 2B**. In case 5 (NMZL), perifollicular cuffs around the atrophic germinal centers appeared to be expanded by monomorphic lymphocytes **Image 2C**. A focally diffuse lymphoid infiltrate in the pericapsular fat (data not shown), outside of the architecturally preserved lymph node, was also noted in this case. In case 6 (LBCL), close examination of a focally expanded interfollicular area identified infiltration by large cells **Image 2D**. These large cells had round to oval nuclei 2 to 3 times the size of small lymphocytes, with vesicular chromatin, variably prominent nucleoli, and moderate to ample amounts of clear cytoplasm (Image 2D, inset). Reed-Sternberg cells or variants were not seen. Fibrosis was prominent between the follicles (Image 2D), and the capsule was thickened, but the area with large cell infiltration did not show fibrosis.

All 23 cases of diagnostic HV-CD showed mostly preserved lymphoid architecture with increased lymphoid follicles containing atrophic or variably regressed germinal centers, hyaline deposits, and vascular penetration **Image 3A**. All cases had well-defined mantle zones, and broad mantle zones with concentric arrangement of mantle zone cells (Image 3A) **Image 3B** were noted in 19 cases (83%). Increased vascularity and variable plasmacytosis were found in the interfollicular areas of all cases.

Immunohistochemical Analysis and ISH for EBER

All 6 cases of B-cell lymphoma with HV-CD–like features had increased lymphoid follicles highlighted by B-cell antigen markers **Image 4A**, **Image 4B**, **Image 4C**, **Image 4D**, and **Image 4E**, including CD20, CD79a, and/or PAX5. Particularly, in cases 1 and 2 (FL), large cells in the follicle centers were positive for CD20 (Image 4B) but negative for CD21. BCL2 staining was performed in both cases: it was positive in the germinal center large cells in case 1 **Image 4F** but negative in case 2 **Image 4G**. In case 2, anti-Ki-67 revealed a relatively low proliferation rate in germinal centers **Image 4H**, but immunoreactivity was focally increased in some germinal centers with up to 50% of the cells stained. Of note, a sharp border between germinal center and mantle zone cells, which is usually seen in reactive follicular hyperplasia, was not demonstrated by Ki-67 or BCL2 staining in cases 1 and 2. Ki-67 staining was also performed in cases 3, 4, and 5 and highlighted a high proliferation rate in germinal centers but a relatively low number of cells staining in the mantle zone and interfollicular areas **Image 4I**.

In case 3 (MCL), CD5 staining showed partial, weak reactivity in the mantle zones. Anti-BCL2 was positive in the mantle zones and interfollicular cells (T cells) but negative in germinal centers. BCL6 staining showed the opposite pattern, marking germinal center cells. The mantle zones also stained for cyclin D1 **Image 4J** and had a low proliferation rate (<5% cells).

CD3 and CD5 stains highlighted a predominance of T cells in interfollicular areas in cases 1, 2, and 3, whereas B-cell antigen markers demonstrated increased numbers of

DOI: 10.1309/AJCPF5AESY7OWIXF

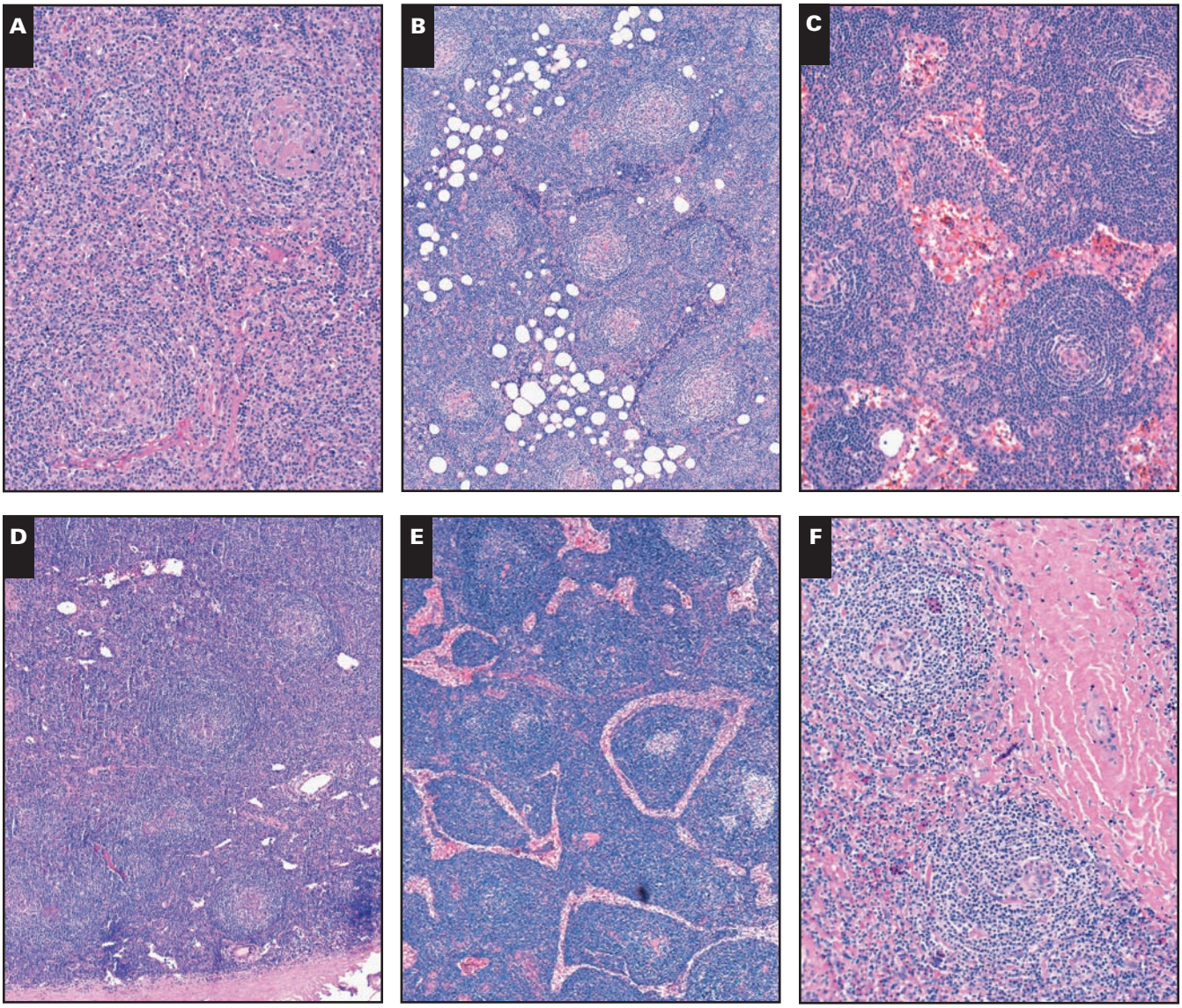

Image 1 Histologic features of B-cell lymphoma with hyaline vascular Castleman disease–like changes. **A** (Case 1), Follicular lymphoma (FL) (H&E, ×100). **B** (Case 2), FL (H&E, ×40). **C** (Case 3), Mantle cell lymphoma (H&E, ×100). **D** (Case 4), Nodal marginal zone lymphoma (NMZL) with follicular colonization (H&E, ×40). **E** (Case 5), NMZL (H&E, ×40). **F** (Case 6), Focal large B-cell lymphoma (H&E, ×100). Note the increased lymphoid follicles with atrophic germinal centers, hyaline deposits, vascular penetration, and an increase in interfollicular vascularity in each case. Expanded mantle zones or perifollicular zones are best seen in cases 3 (**C**) and 5 (**E**), with concentric arrangement of mantle zone cells noted only in case 3 (**C**). Dilated sinusoids with prominent histiocytosis are seen in cases 3 (**C**) and 5 (**E**), whereas case 6 (**F**) shows marked perifollicular/interfollicular fibrosis.

B cells in perifollicular/marginal zone areas in cases 4 and 5 (NMZL; Images 4D and 4E) and focal large cell infiltrates in interfollicular areas in case 6. In case 4, B-cell antigen markers, including CD20, CD79a, PAX5, OCT2, and BOB.1, stained large cells in many germinal centers, in addition to lymphocytes in the perifollicular/marginal zone (Image 4D). These results excluded the possibility of dysplastic follicular dendritic cells and confirmed the B-cell lineage of the large cells in germinal centers. Staining for germinal center markers CD10 and BCL6 was negative in the germinal centers in this case, whereas BCL2 was positive, supporting the neoplastic nature of the follicular infiltrates. A similar immunophenotypic profile was seen in the perifollicular/marginal zone, and, thus, the findings were compatible with a nodal marginal zone B-cell lymphoma with follicular colonization. The intervening presence of spared mantle zones generated a target-like growth pattern, best seen by MUM1 **Image 5A** and Ki-67 staining **Image 5B**. Anti-CD138 highlighted increased plasmacytoid lymphocytes in the interfollicular areas that were κ light chain–restricted **Image 5C** and **Image 5D**.

DOI: 10.1309/AJCPF5AESY7OWIXF

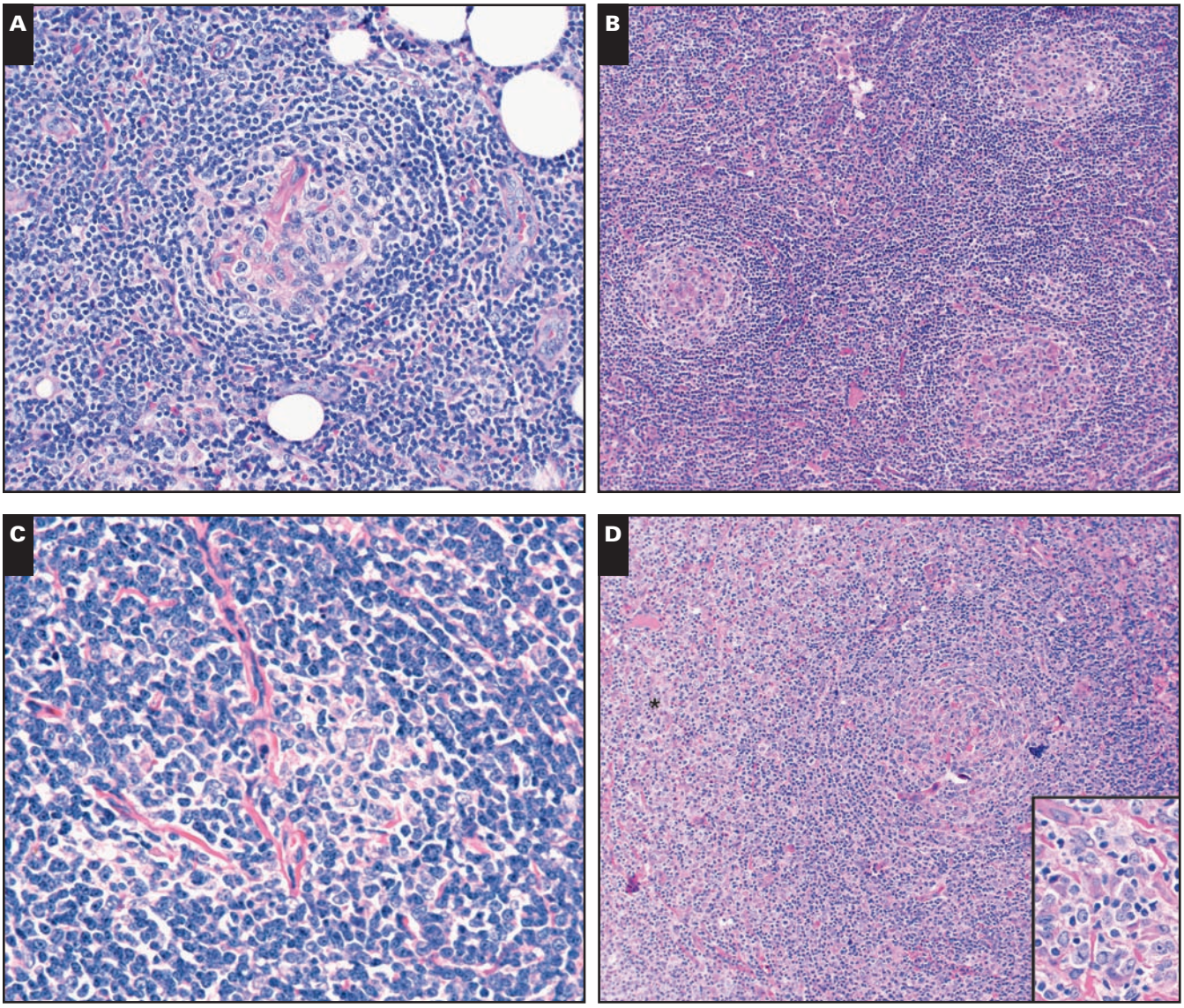

Image 2 Subtle histologic changes suggestive of an occult lymphoid neoplasm in B-cell lymphomas with hyaline vascular Castleman disease–like changes. **A** (Case 2), Follicular lymphoma. Note the relatively monomorphic large cells with vesicular chromatin in an atrophic germinal center with hyaline vascular penetration; there is an ill-defined border between the germinal center and cuffing mantle zone (H&E, ×200). **B** (Case 4), Nodal marginal zone lymphoma (NMZL) with follicular colonization. Note the increased medium-sized to large cells with clear cytoplasm in the germinal centers and the perifollicular area (H&E, ×100). **C** (Case 5), NMZL. Note the monotonous population of small, mature-appearing lymphocytes around ill-defined germinal centers with vascular penetration (H&E, ×400). **D** (Case 6), Focal large B-cell lymphoma. * Focal increased large cells in an interfollicular area in proximity to an involuted germinal center with hyaline vascular penetration (H&E, ×200). Inset, Shows close inspection of focal expanded interfollicular area (*). Note the increased large cells with vesicular chromatin and abundant clear cytoplasm (H&E, ×400).

In contrast, case 5 demonstrated positive immunoreactivity to anti-BCL2 in perifollicular cuffs, but with absence of staining in germinal centers, which were positive for CD10 and BCL6. The lymphocytes in the perifollicular cuffs were negative for CD5 and cyclin D1. The proliferation rate was low except for increased Ki-67 labeling in the atrophic germinal centers (Image 4I).

In case 6 (focal LBCL), large cells in the focally expanded interfollicular areas stained for CD45, CD20 **Image 5E**, CD79a, and PAX-5. They were also positive for CD30 and BCL2 but were negative for CD15, CD10, and BCL6. CD23 highlighted follicular dendritic meshworks in follicular areas, while no well formed follicular dendritic meshworks were noted in the expanded interfollicular areas containing the large cell infiltrate.

DOI: 10.1309/AJCPF5AESY7OWIXF

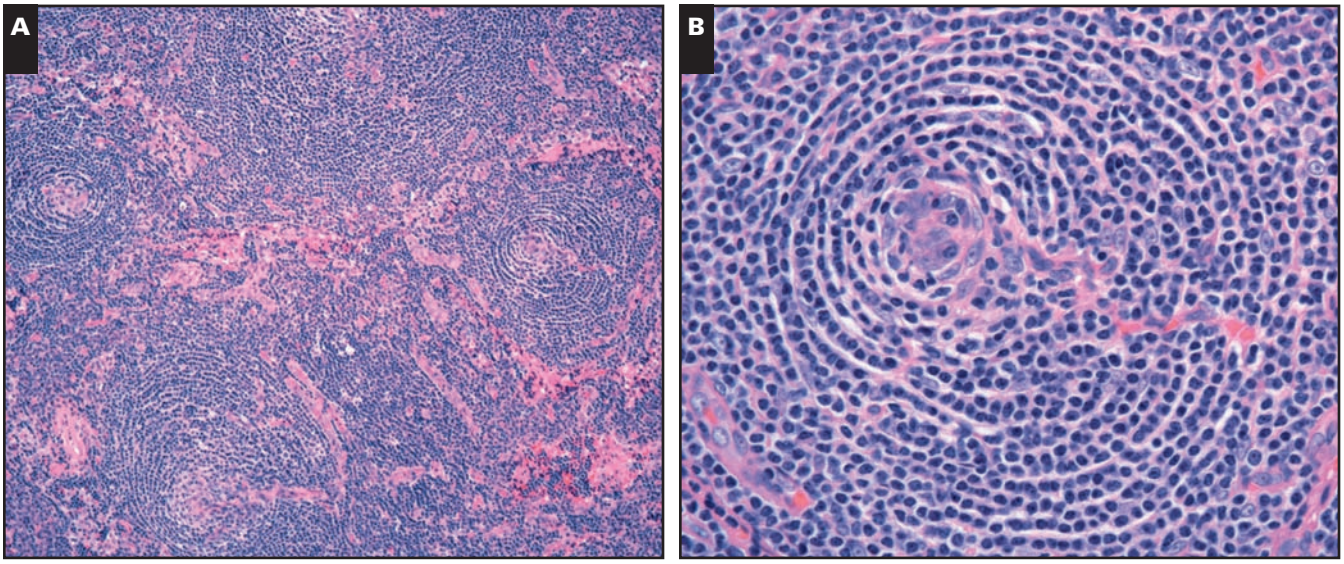

Image 3 Characteristic histologic features in a case of diagnostic hyaline vascular Castleman disease. **A**, Increased lymphoid follicles with atrophic germinal centers, hyaline vascular penetration, and increased vascularity in the interfollicular area (H&E, ×100). **B**, High magnification of a follicle with an atrophic germinal center and hyaline vascular penetration (H&E, ×400). Expanded mantle zones with concentric arrangement of lymphocytes are well appreciated in **A** and **B**.

Anti-HHV-8 staining was performed in 4 cases (cases 1, 3, 4, and 6) and was negative in all 4 cases. Anti-IgG4 staining was also performed and demonstrated no increase in IgG4+ plasma cells in any of the cases stained for this marker (cases 1, 3, 4, and 6).

ISH for EBER was performed in 5 cases of B-cell lymphoma with HV-CD–like features (cases 1 and 3-6), and all were negative for the viral RNA.

Immunohistochemical stains were performed in only 8 cases of diagnostic HV-CD owing to the presence of characteristic morphologic features, negative flow cytometric results, and/or low clinical suspicion for lymphoma. Overriding features in these cases were increased follicles (highlighted by B-cell antigen markers) **Image 6A** and an increase in T cells and plasma cells (anti-CD138 stain) in interfollicular areas. Of note, extremely atrophic germinal centers showed depletion of CD20+ B cells in these germinal centers (Image 6A, arrows). All cases assessed for κ and λ light chain expression by immunostaining demonstrated polyclonal plasmacytosis. Follicle centers were negative for BCL2 **Image 6B**, and mantle zones were negative for cyclin D1 **Image 6C**. Anti-Ki-67 typically revealed a relatively high proliferation rate in the majority of germinal centers **Image 6D**, although extremely atrophic germinal centers usually showed lower labeling, in keeping with anti-CD20 staining. In addition, highly proliferative germinal centers showed sharp borders with surrounding hypoproliferative mantle zones in the majority of lymphoid follicles (Image 6D). Correspondingly, a sharp border between germinal center and mantle zone was also highlighted by BCL2 staining, in which a positive mantle zone demarcated a negative germinal center (Image 6B). Anti-CD21 or anti-CD23 highlighted well-formed follicular dendritic meshworks and showed staining of some large follicular dendritic cells in germinal centers at high magnification. We stained 6 cases for anti-HHV-8, and all were negative.

Flow Cytometric Analysis

Concurrent flow cytometric analysis was performed in all cases of B-cell lymphoma with HV-CD–like features. Of these, 3 cases (case 2, 3, and 5) demonstrated a monoclonal B-cell population, supporting a diagnosis of B-cell lymphoma. In case 2 (FL), the monoclonal B-cell population expressed CD10, suggesting a follicle center origin for the B-cell neoplasm. Case 3 (MCL) showed coexpression of CD5 and κ light chain in monoclonal B cells, which were negative for CD10 and CD23, and constituted approximately 6% of all analyzed events. A monoclonal B-cell population was identified in case 5, expressing λ light chain and showing negativity for CD5, CD10, and CD23. In cases 1, 4, and 6, concurrent flow cytometric analysis showed a polyclonal B-cell population with no subpopulation of abnormal B cells detected. However, in case 1, subsequent flow cytometric analysis at the time of recurrent cervical lymphadenopathy detected a monoclonal B-cell population with CD10 coexpression.

Of 23 cases of diagnostic HV-CD, 12 had concurrent flow cytometric analysis performed, and all demonstrated polyclonal B-cell populations.

DOI: 10.1309/AJCPF5AESY7OWIXF

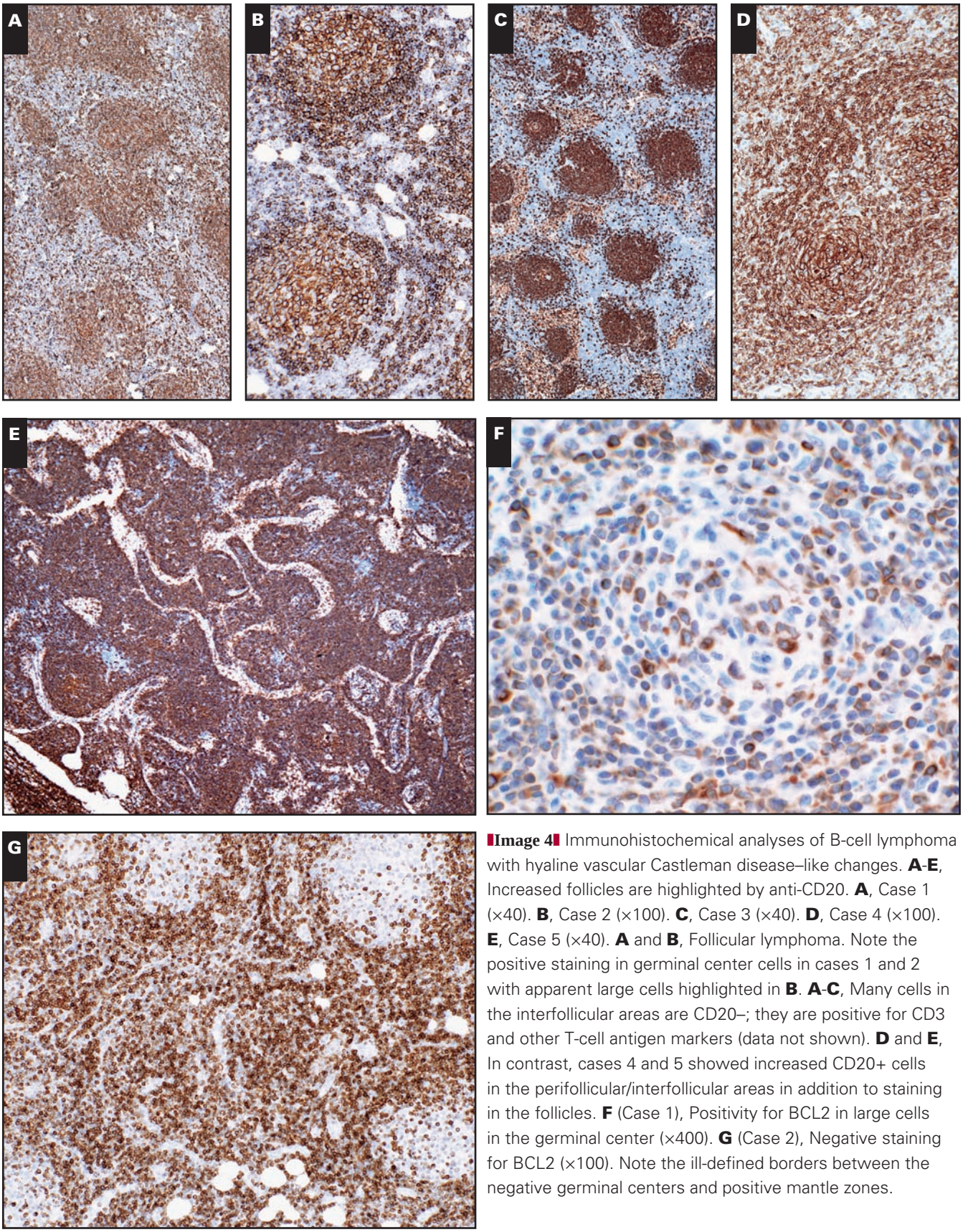

Image 4 Immunohistochemical analyses of B-cell lymphoma with hyaline vascular Castleman disease–like changes. **A**-**E**, Increased follicles are highlighted by anti-CD20. **A**, Case 1 (×40). **B**, Case 2 (×100). **C**, Case 3 (×40). **D**, Case 4 (×100). **E**, Case 5 (×40). **A** and **B**, Follicular lymphoma. Note the positive staining in germinal center cells in cases 1 and 2 with apparent large cells highlighted in **B**. **A**-**C**, Many cells in the interfollicular areas are CD20–; they are positive for CD3 and other T-cell antigen markers (data not shown). **D** and **E**, In contrast, cases 4 and 5 showed increased CD20+ cells in the perifollicular/interfollicular areas in addition to staining in the follicles. **F** (Case 1), Positivity for BCL2 in large cells in the germinal center (×400). **G** (Case 2), Negative staining for BCL2 (×100). Note the ill-defined borders between the negative germinal centers and positive mantle zones.

DOI: 10.1309/AJCPF5AESY7OWIXF

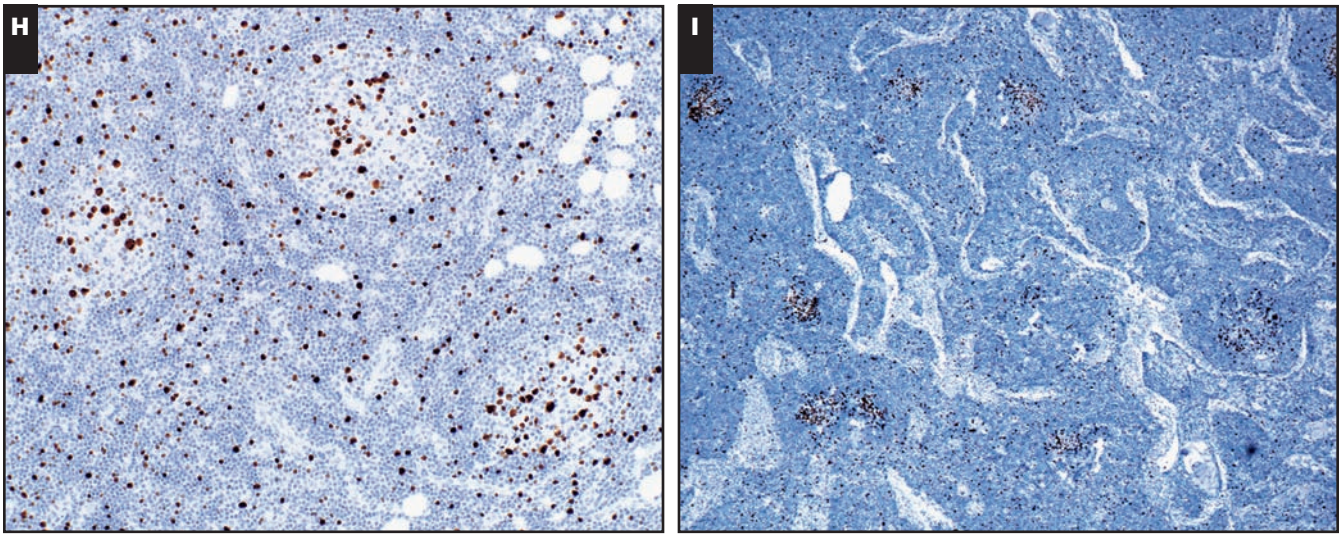

Image 4 (cont) **H** (Case 2), Note the relatively low proliferation index and random distribution of positive cells in germinal centers (anti-Ki-67, ×100). **I**, Case 5 (anti-Ki-67, ×40). **J** (Case 3), Positive anti–cyclin D1 staining in the mantle zones (×100).

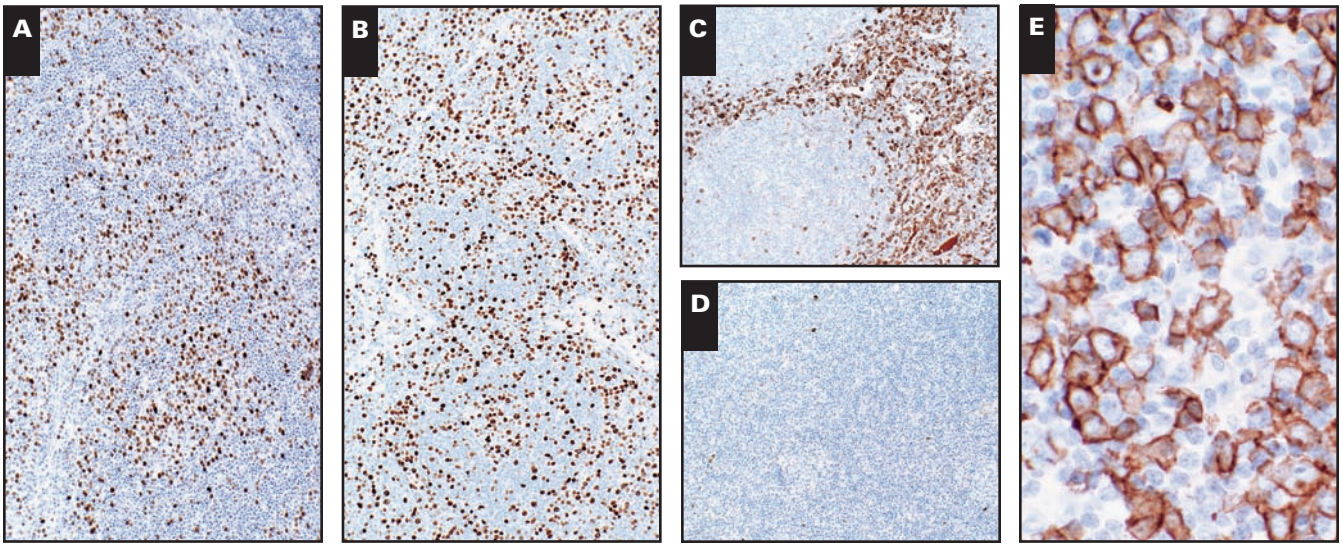

Image 5 Immunohistochemical analyses of B-cell lymphoma with hyaline vascular Castleman disease–like changes. **A**-**D**, Case 4 (**A**, anti-MUM1, ×100; **B**, anti-Ki-67, ×100; **C**, anti–κ light chain, ×100; **D**, anti–λ light chain, ×100). Note the targetoid arrangement of positive cells highlighted by anti-MUM1 (**A**) and anti-Ki-67 (**B**) with clustered positive cells in germinal centers and in perifollicular/interfollicular areas, separated by much lower stained mantle zones. Also note the apparently κ light chain–restricted plasmacytoid cells in the interfollicular area (**C**) compared with λ light chain stain (**D**). **E** (Case 6), Positive anti-CD20 staining in large cells (×400; * in Image 2D).

DOI: 10.1309/AJCPF5AESY7OWIXF

Cytogenetic and Molecular Studies

Interphase FISH analysis was performed in 5 cases of B-cell lymphoma with HV-CD–like features. In case 1 (FL), FISH analysis revealed no evidence for t(14;18) *IGH/BCL2* fusion but demonstrated *BCL6* rearrangement, a variant gene rearrangement seen occasionally in FL. In case 2 (FL), while no lymph node tissue material was available for additional tests, FISH for t(14;18) *IGH/BCL2* on a staging bone marrow aspirate showed a fusion signal in a small number of interphase cells, consistent with low-level involvement by FL. Case 3 (MCL) demonstrated fusion of the *CCND1/IGH* genes in 12% of interphase cells by FISH **Image 7**, confirming the diagnosis of MCL. In case 4 (NMZL), FISH for *IGH/BCL2* fusion and rearrangement of *MALT1* and *BCL6* showed no evidence of rearrangements at these loci, but instead revealed signal patterns consistent with 3 copies of *BCL2*, *MALT1*, and *BCL6* loci in 14% to 33% of cells, suggesting possible trisomy of chromosomes 3 (*BCL6*) and 18 (*BCL2*, *MALT1*). In case 5 (NMZL), despite the lack of cyclin D1 and CD5 positivity by immunostains, the B-cell lymphoma had a conspicuously nodular growth pattern with monomorphic appearance, raising the possibility of MCL. However, FISH for *CCND1/IGH*

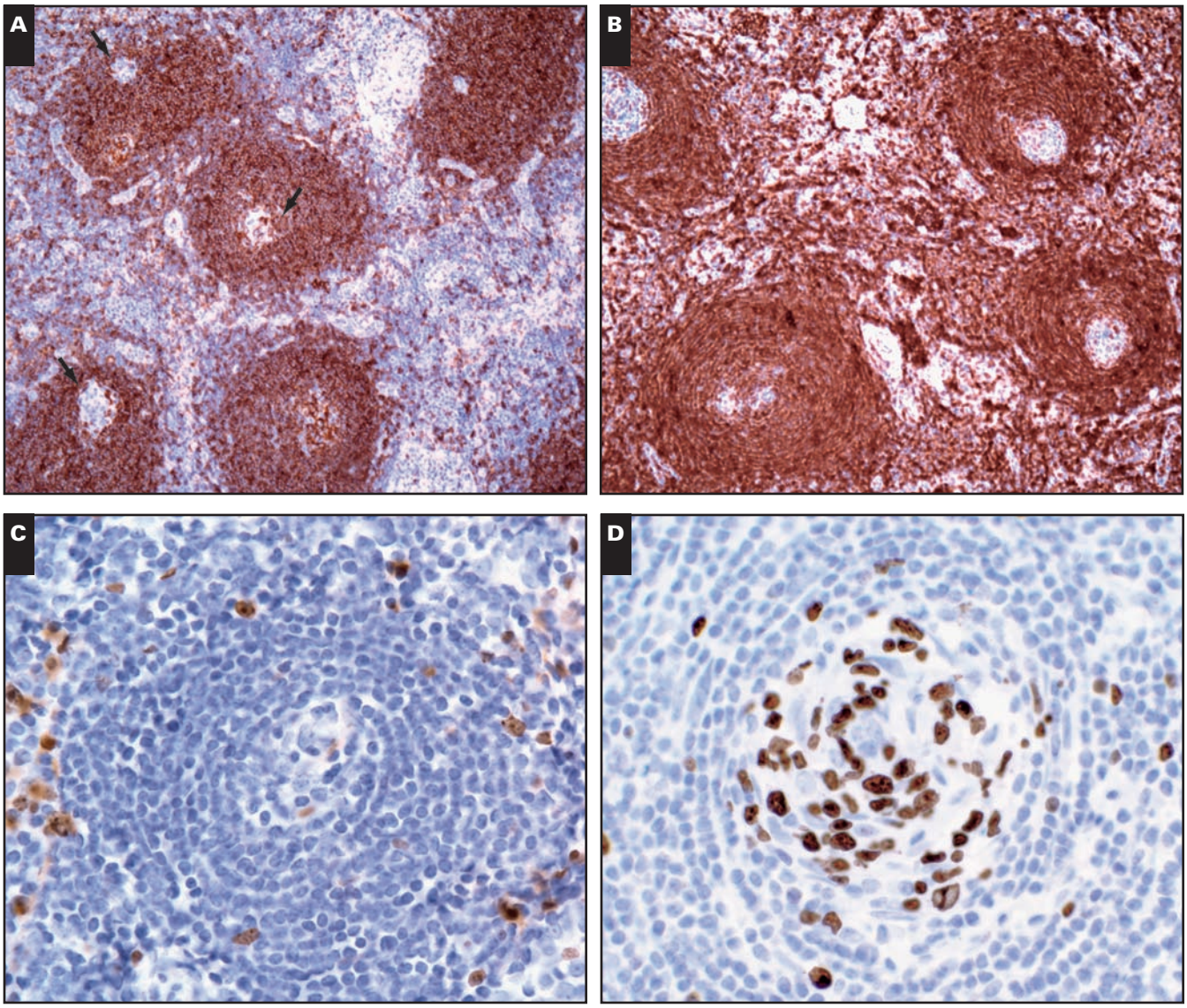

Image 6 Immunohistochemical features of diagnostic hyaline vascular Castleman disease. **A**, Note staining in follicles but markedly decreased staining in an extremely atrophic germinal center (arrows) and numerous negative cells (T cells and plasma cells) in the interfollicular area (anti-CD20, ×100). **B**, Note the negative atrophic germinal centers with sharp borders from a positive mantle zone in contrast with the blurred borders seen in Image 4G (anti-BCL2, ×100). **C**, Note the negative staining in the mantle zone in contrast with the positive reactivity in Image 4J (anti–cyclin D1, ×400). **D**, A relatively increased proliferation index is seen in the germinal center, although it is apparently atrophic; the border between the positive germinal center and the mantle zone is sharp rather than ill-defined, as seen in Image 4H (anti-Ki-67, ×400).

DOI: 10.1309/AJCPF5AESY7OWIXF

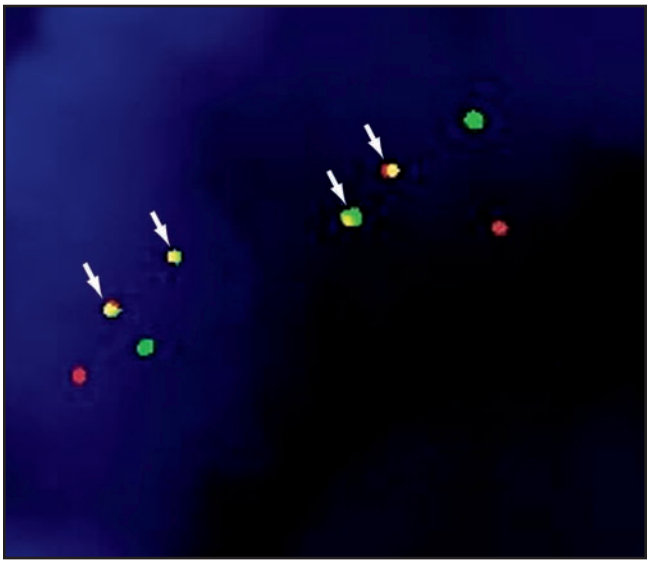

Image 7 (Case 3) *CCND1/IGH* fusion gene detected by dual-color, double-fusion interphase fluorescence in situ hybridization analysis. Note the positive cells each with 2 fusions of red and green fluorescent signals (arrows), representing cells harboring fusion of the *CCND1* and *IGH* genes. An isolated red signal and isolated green signal represent intact *CCND1* (red) and intact *IGH* (green) genes, respectively, in each of the cells. Image courtesy of Pauline Brenholz, MD, Genzyme Genetics, New York, NY.

was negative, effectively excluding this possibility, and a diagnosis of NMZL with HV-CD–like changes was made.

Gene rearrangement studies demonstrated clonal *IGH* gene rearrangement in cases 4 and 6 but were indeterminate in case 1. B-cell clonality studies by PCR were not performed in cases 2, 3, and 5 because monoclonal B-cell populations were already apparent by flow cytometric analysis.

Only 4 cases of diagnostic HV-CD had *IGH* gene rearrangement studies performed, and all were negative for clonal rearrangement. No FISH analysis was performed on these cases.

Clinical Course

There was clinical follow-up for 5 of 6 cases of B-cell lymphoma with HV-CD–like features, but this was long-term in only 2 cases (case 1 and 6). In case 1, the patient received 6 cycles of R-CHOP, followed by 3 cycles of rituximab, ifosfamide, carboplatin, and etoposide (also called RICE) and carmustine with complete response. The patient in case 6 was treated with R-CHOP for 6 cycles, with consolidative radiotherapy to the residual left upper quadrant mass, resulting in complete response. Both patients were alive up to the time when this article was prepared, although 1 patient (case 1) had a recent relapse with evidence of large cell transformation. Patients in cases 2, 4, and 5 were recently diagnosed without sufficient follow-up to date. The patient in case 3 was not treated owing to debilitated status.

Of 23 cases of diagnostic HV-CD, 13 had clinical follow-up ranging from 1 to 96 months (median, 10 months). All of these cases showed resolution of clinical symptoms after surgical excision of the lesions, and no progression of disease was seen on follow-up evaluations.

Discussion

CD, when associated with lymphoma, most often manifests as the multicentric/PC type. In contrast, the HV variant is usually a benign, localized (unicentric) lump or mass, and any associated symptoms typically resolve following surgical removal of the solitary lesion. The association with lymphoma is uncommon in HV-CD, and HV-CD–like change in tissue sites concurrently involved by lymphoma is rare. Rare cases of the latter type have been reported, mostly in the setting of classical and nodular lymphocyte predominant Hodgkin lymphoma[4-6] and FL.[10-14] Nevertheless, other types of B-cell lymphoma have been described to coexist infrequently with HV-CD–like changes, including diffuse large B-cell lymphoma,[15] HHV-8+ LBCL,[16] and MCL.[4]

Herein we report a heterogeneous group of B-cell lymphomas in which the neoplastic process was masked by changes characteristic of HV-CD, leading to a potential misdiagnosis. As such, the histologic findings were beyond the occasional involuted follicles that can be seen nonspecifically in some reactive and neoplastic conditions. Instead, the majority of the follicles in all 6 cases of our series were regressed, with prominent hyaline deposits and vascular penetration, preserved mantle zones, and increased interfollicular vascularity, features classically associated with HV-CD. The preserved nodal architecture with widely spaced follicles and intact mantle zones suggested a reactive rather than neoplastic process. Indeed, initial morphologic evaluation led to a consideration of HV-CD in all cases of the current series, illustrating the potential diagnostic pitfall that can occur. In fact, case 1 (Table 1) was diagnosed as HV-CD on biopsy of an enlarged cervical lymph node at initial diagnosis, largely owing to a negative concurrent flow cytometric result and the deceptive HV-CD–like histologic changes. However, persistent clinical symptoms and recurrent cervical lymphadenopathy shortly after the first lymph node excision prompted another biopsy, which demonstrated similar morphologic features, but, at this point, a monoclonal B-cell population with CD10 coexpression was detected by flow cytometric analysis. The original case was reevaluated, and a diagnosis of FL was made.

Despite the histologic features suggesting HV-CD, all 6 patients with B-cell lymphoma with HV-CD–like changes had multiple sites of lymphadenopathy, and the majority (5/6)

DOI: 10.1309/AJCPF5AESY7OWIXF

had systemic symptoms, clinically suggestive of multicentric CD or lymphoma. In contrast, none of the patients with diagnostic HV-CD in our control group had lymphadenopathy or involvement of tissue sites other than the presenting lesions (Table 2). Therefore, a clinical history of lymphoma, systemic symptoms, and generalized lymphadenopathy are atypical findings for HV-CD that should raise suspicion for a lymphomatous process and prompt additional studies to exclude the possibility of an occult lymphoid neoplasm. While B-cell lymphomas in our limited series tended to occur in older patients (median age, 69 years), in contrast with a younger population in diagnostic HV-CD (median age, 25 years), a significant overlap was present between the 2 groups (range, 40-86 in B-cell lymphoma vs 11-85 in HV-CD; Table 2), precluding its use as a distinctive factor.

In most if not all of these cases of B-cell lymphoma with HV-CD–like features, subtle histologic clues were present that should raise suspicion and prompt additional testing to allow distinction from HV-CD. For example, close inspection of germinal centers in the FL cases (cases 1 and 2) revealed large cells with a greater degree of monomorphism than typically associated with reactive germinal centers. Immunohistochemical staining for BCL2 was helpful in case 1, in which the malignant centroblasts were aberrantly positive for this diagnostic marker (Image 4F). However, as demonstrated in case 2 (Image 4G), this immunostain can often be misleading in cases of BCL2– FL. Because many BCL2– FLs are grade 3 lesions, the follicles in these cases are composed of predominantly large centroblasts; thus, cytologic atypia with increased large cells should raise suspicion for a neoplastic process, particularly FL. A Ki-67 stain may be useful in these cases by assessing the presence or absence of polarity and the degree of demarcation of follicle center/mantle zone margins. Both FL cases showed somewhat random distribution of Ki-67+ cells in follicles that had no polarity or demarcated borders with mantle zones (Image 4H). It should also be kept in mind that dysplastic follicular dendritic cells are not uncommonly encountered in the atrophic follicles of HV-CD,[3] thus necessitating immunohistochemical delineation of cell lineage with B-cell antigen markers (eg, CD20, CD79a, and PAX5) and follicular dendritic cell antigen markers (CD21 and CD23).

In addition to the atrophic germinal centers, the interfollicular areas in suspected cases of HV-CD should be examined closely for atypical findings, such as Reed-Sternberg cells or variants, clusters of large cells, or atypical mixed infiltrates that could raise the possibility of Hodgkin lymphoma, LBCL, or NMZL, respectively. Immunohistochemical analysis should be performed in suspicious cases with B- and T-cell antigen markers. In cases of diagnostic HV-CD, T cells comprise the predominant population in perifollicular/interfollicular areas, as observed in our control cases; thus, any increase in interfollicular B cells should prompt additional testing to exclude the possibility of a B-cell lymphoma, such as NMZL. Indeed, in cases 4 and 5 of our series, immunohistochemical analysis revealed increased interfollicular/perifollicular B cells, suggesting an NMZL. The neoplastic nature was confirmed by FISH analysis and *IGH* gene rearrangement study in case 4 and by flow cytometric immunophenotyping in case 5. In case 6, focal large cell infiltrates noted in the interfollicular areas were positive for B-cell antigen markers (CD20, CD79a, and PAX5), raising the possibility of an LBCL, which was supported by clonal rearrangement of *IGH* detected by PCR. While focal LBCL with HV-CD–like changes has been described in a case report,[15] NMZL with histologic features reminiscent of HV-CD has not been reported in the English literature.

Of particular interest is case 3, which displayed morphologic features essentially indistinguishable from HV-CD. It demonstrated all the essential histologic features of HV-CD, including concentric arrangement of lymphocytes in expanded mantle zones. Therefore, this case is representative of a major diagnostic challenge that can occur in rare cases of MCL. The mantle zone pattern of MCL has been well documented,[17] but cases closely resembling HV-CD are extremely rare. We found only scarce references describing possible cases of coexisting HV-CD and MCL, without pathologic details, in the English literature.[4,18] Further complicating the issue, benign mantle zone hyperplasia is characteristic of HV-CD (83% in our control cases). Cases of HV-CD with prominent mantle zone expansion have been referred to as the "lymphoid variant," containing pale cuffs of mantle zone cells,[19] or as the "follicular variant, primary follicular pattern."[20] Such cases demonstrate the typical features of HV-CD, but additionally have increased density of follicles and large nodules of mantle cells. Because there is considerable morphologic overlap, MCL should specifically be excluded in cases with these morphologic features, by immunohistochemical staining for cyclin D1 and/or FISH analysis for the hallmark *CCND1/IGH* fusion gene. Immunohistochemical evaluation for CD5 coexpression in the mantle zones is not sufficient because coexpression of CD5 is usually low in MCL, as illustrated by our case with equivocal staining of anti-CD5 in mantle zone lymphocytes, and it is well known that benign mantle zone lymphocytes in HV-CD can have weak CD5 and BCL2 expression.[21]

Hypothetically, each of these cases, other than case 4, may represent an "in situ" pattern of involvement in which the lymphoma partially involved structures of an otherwise architecturally preserved lymph node. As such, the neoplastic cells were most prominent in germinal centers in cases 1 and 2 (FL), mantle zones in case 3 (MCL), the marginal zone in case 5 (NMZL), and a focal interfollicular area in case 6 (LBCL of post–germinal center origin). Analogous to in situ lesions in nonhematopoietic neoplasms, in situ localization of lymphoma creates a diagnostic challenge. Flow cytometry is an

DOI: 10.1309/AJCPF5AESY7OWIXF

important tool for the diagnosis of non-Hodgkin lymphoma, and it is particularly sensitive and specific for the diagnoses of small B-cell lymphomas. However, a significant proportion of the cases in our series had negative flow cytometric results (3 of 6 cases), which may be explained by in situ localization or partial involvement by B-cell lymphoma, further emphasizing the need for a multifaceted approach when dealing with these unusual cases.

The pathogenesis of HV changes in CD and the causes of the prominent HV-CD–like changes associated with B-cell lymphomas are not well understood. Based on our series, there does not seem to be a particular association with immunodeficiency, autoimmune disease, HHV-8 or EBV infection, or an IgG4-related disease. Whether interplay between cytokines derived from the neoplastic cells and the microenvironment of lymphoid tissue occurs and whether the presence of prominent HV-CD changes in B-cell lymphomas has a distinctive etiologic association, therapeutic implication, and/or prognostic significance is unclear and remains to be further determined.

This study confirms that HV-CD is a diagnosis of exclusion, and a number of B-cell lymphomas, along with other reactive and neoplastic conditions, can have a similar morphologic appearance. Indeed, B-cell lymphomas can involve any of the lymph node compartments that show HV-CD features, including the atrophic germinal centers (FL), expanded mantle zones (MCL), and interfollicular areas (NMZL and focal LBCL). Each of these compartments should be evaluated closely with judicious use of a variety of ancillary tests, as needed, and in combination with the clinical history and manifestations to exclude the possibility of an occult lymphoma.

From the Departments of Pathology, [1]University of Southern California-Los Angeles County Medical Center; and [2]Duke University Medical Center, Durham, NC.

Presented in part at the XV Biannual Meeting of the European Association for Haematopathology; September 25-30, 2010; Uppsala, Sweden.

Address reprint requests to Dr Wang: Dept of Pathology, DUMC Box 3712, M-345 Davison Bldg (Green Zone), Duke Hospital South, Durham, NC 27710.

Acknowledgment: We thank Steven R. Conlon, Department of Pathology, Duke University School of Medicine, for technical assistance with the photo images.

References

1. Castleman B, Iverson L, Menendez VP. Localized mediastinal lymphnode hyperplasia resembling thymoma. *Cancer*. 1956;9:822-830.
2. Keller AR, Hochholzer L, Castleman B. Hyaline-vascular and plasma-cell types of giant lymph node hyperplasia of the mediastinum and other locations. *Cancer*. 1972;29:670-683.
3. Cronin DM, Warnke RA. Castleman disease: an update on classification and the spectrum of associated lesions. *Adv Anat Pathol*. 2009;16:236-246.
4. Larroche C, Cacoub P, Soulier J, et al. Castleman's disease and lymphoma: report of eight cases in HIV-negative patients and literature review. *Am J Hematol*. 2002;69:119-126.
5. Zarate-Osorno A, Medeiros LJ, Danon AD, et al. Hodgkin's disease with coexistent Castleman-like histologic features: a report of three cases. *Arch Pathol Lab Med*. 1994;118:270-274.
6. Drut R, Larregina A. Angiofollicular lymph node transformation in Hodgkin's lymphoma. *Pediatr Pathol*. 1991;11:903-908.
7. Harris NL, Swerdlow SH, Jaffe ES, et al. Follicular lymphoma. In: Swerdlow SH, Campo E, Harris NL, et al, eds. *WHO Classification of Tumours of Haematopoietic and Lymphoid Tissues*. 4th ed. Lyon, France: IARC Press; 2008:220-226.
8. Swerdlow SH, Campo E, Seto M, et al. Mantle cell lymphoma. In: Swerdlow SH, Campo E, Harris NL, et al, eds. *WHO Classification of Tumours of Haematopoietic and Lymphoid Tissues*. 4th ed. Lyon, France: IARC Press; 2008:229-232.
9. Campo E, Pileri SA, Jaffe ES, et al. Nodal marginal zone lymphoma. In: Swerdlow SH, Campo E, Harris NL, et al, eds. *WHO Classification of Tumours of Haematopoietic and Lymphoid Tissues*. 4th ed. Lyon, France: IARC Press; 2008:218-219.
10. Vasef M, Katzin WE, Mendelsohn G, et al. Report of a case of localized Castleman's disease with progression to malignant lymphoma. *Am J Clin Pathol*. 1992;98:633-636.
11. Kojima M, Matsumoto M, Miyazawa Y, et al. Follicular lymphoma with prominent sclerosis ("sclerosing variant of follicular lymphoma") exhibiting a mesenteric bulky mass resembling inflammatory pseudotumor: report of three cases. *Pathol Oncol Res*. 2007;13:74-77.
12. Warnke RF, Weiss LM, Chan JKC, et al. *Tumors of the Lymph Nodes and Spleen*. Bethesda, MD: Armed Forces Institute of Pathology; 1995:63-118. *Atlas of Tumor Pathology*; Third series; Fascicle 14.
13. Nozawa Y, Hirao M, Kamimura K, et al. Unusual case of follicular lymphoma with hyaline-vascular follicles [letter]. *Pathol Int*. 2002;52:794-795.
14. Kojima M, Sakurai S, Isoda A, et al. Follicular lymphoma resembling with hyaline-vascular type of Castleman's disease: the morphologic and immunohistochemical findings of two cases. *Cancer Ther*. 2009;7:109-112.
15. Erkurt MA, Aydogdu I, Kuku I, et al. A multicentric, hyaline vascular variant of Castleman's disease associated with B cell lymphoma: a case report. *Cases J*. 2009;2:8183. doi:10.4076/1757-1626-2-8183.
16. Ferry JA, Sohani AR, Longtine JA, et al. HHV8-positive, EBV-positive Hodgkin lymphoma–like large B-cell lymphoma and HHV8-positive intravascular large B-cell lymphoma. *Mod Pathol*. 2009;22:618-626.
17. Yatabe Y, Suzuki R, Matsuno Y, et al. Morphological spectrum of cyclin D1–positive mantle cell lymphoma: study of 168 cases. *Pathol Int*. 2001;51:747-761.
18. Soulier J, Grollet L, Oksenhendler E, et al. Molecular analysis of clonality in Castleman's disease. *Blood*. 1995;86:1131-1138.
19. Kojima M, Nakamura S, Iijima M, et al. Lymphoid variant of hyaline vascular Castleman's disease containing numerous mantle zone lymphocytes with clear cytoplasm. *APMIS*. 2005;113:75-80.
20. Kojima M, Shimizu K, Ikota H, et al. "Follicular variant" of hyaline-vascular type of Castleman's disease: histopathological and immunohistochemical study of 11 cases. *J Clin Exp Hematopathol*. 2008;48:39-45.
21. Peh SC, Shaminie J, Poppema S, et al. The immunophenotypic patterns of follicle centre and mantle zone in Castleman's disease. *Singapore Med J*. 2003;44:185-191.

DOI: 10.1309/AJCPF5AESY7OWIXF

HOLOGIC®

First and Only FDA Cleared
Digital Cytology System

Genius™ Cervical AI

Genius™ Review Station

Genius™ Digital Imager

Empower Your Genius With Ours

Make a Greater Impact on Cervical Cancer
with the Advanced Technology of the
Genius™ Digital Diagnostics System

Click or Scan
to discover more

genius™
DIGITAL DIAGNOSTICS